

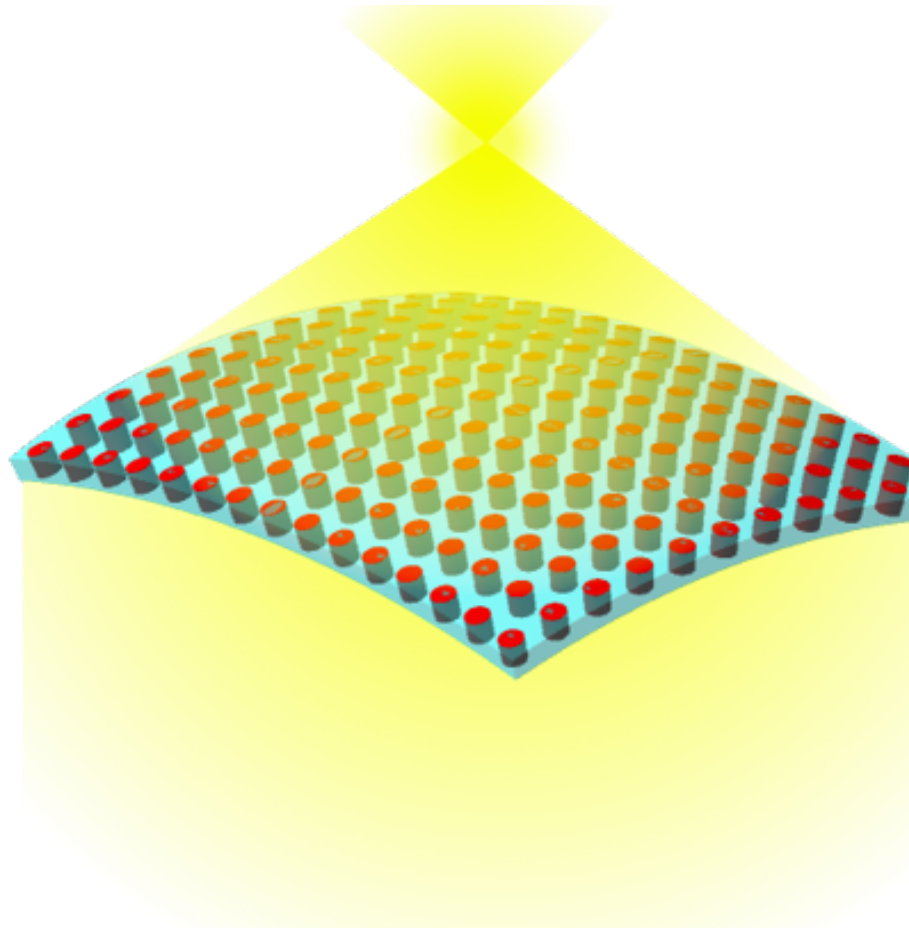
# Rapid fabrication of curved metasurfaces through wafer grinding

Robert Lupoiu, Chenkai Mao, Yixuan Shao

June 18, 2022

Advisor: Prof. Jonathan Fan

Mentors: J Provine, Swaroop Kommera, Lavendra Mandyam  
E241 Spring 2022



# Contents

<b>1</b>	<b>Introduction</b>	<b>2</b>
1.1	Motivation . . . . .	2
1.2	Benefits to SNF community . . . . .	3
<b>2</b>	<b>Process development and experimentation</b>	<b>4</b>
2.1	Process flow . . . . .	4
2.2	Wafer piece backgrinding . . . . .	6
2.3	Material growth . . . . .	8
2.4	Microstructure patterning . . . . .	11
2.5	Etching and PDMS filling . . . . .	13
2.6	PDMS formulation . . . . .	14
2.7	Precise wafer backgrinding . . . . .	17
2.8	Spin-coating PDMS . . . . .	18
2.9	Molding PDMS . . . . .	21
<b>3</b>	<b>Conclusions and Discussion</b>	<b>27</b>
<b>4</b>	<b>Acknowledgements</b>	<b>27</b>
<b>5</b>	<b>Appendices</b>	<b>28</b>
5.1	Processes developed to facilitate PDMS curing . . . . .	28
5.2	Fine-grinding parameter selection . . . . .	28
5.3	PDMS height via differential drop gauge measurement technique . . . . .	28
5.4	Budget . . . . .	29

# 1 Introduction

## 1.1 Motivation

Elastomer-embedded nanostructures enable classes of devices with functionality beyond that which is possible with the more conventional planar and rigid nanodevices. The utility of nanostructures embedded within flexible elastomers is widely understood in both academia and across industries, enabling devices such as blood cell separators in biomedicine [2] and curved, high-performance conformal metasurfaces in optics. [4] Applications of conformal metasurfaces include phase cloaking, refractive optical element aberration correction, and holographic image projection done by a metasurface conformed to a curved glass surface. [4]

Despite their ability to push the limits of diffractive optics, conformal, elastomer-embedded metasurfaces face major obstacles to widespread industry adoption due to their time-consuming and delicate manufacturing process. The state-of-the-art manufacturing processes demonstrated in the literature thus far embed the metasurface nanostructures in an elastomer that is generally tens of microns thick, which is subsequently released from a handle wafer by wet etching a sacrificial layer of germanium that is generally several hundreds of nanometers thick. [4] This manufacturing process is inherently slow, commonly taking several days to complete, due to a slow sacrificial layer etch rate. This is caused by the restrictively small surface area of sacrificial germanium that is visible to the etchant chemical: a ring that is only several hundreds of nanometers thick. Furthermore, the manufacturing process includes the manual handling of extremely fragile, thin layers of PDMS elastomer, which is extremely difficult to automate for mass-manufactured industrial processes.

In this report, we present experimental results and developed processes that build towards solutions for rapid, mass-manufacturable nanostructures embedded within flexible elastomers. As detailed in Section 2.1, this is achieved through the invention of a molding process that produces thick layers of embedding PDMS material, which is subsequently released using a wafer backgrinder to remove most of the handle wafer.

## 1.2 Benefits to SNF community

The processes developed in this report are of value to researchers working with nanostructures patterned on top of or embedded within flexible materials. Although the focus of this study is on conformal optical metasurfaces, the same process can be used to create high utility devices that have been demonstrated across domains, including biomedicine and materials engineering.

Explicitly, this study assists future research efforts of the SNF community by providing:

1. An SOP and the experimental characterization of using the DISCO Backgrinder, DAG810, for the processing of wafer pieces.
2. The experimental characterization of the hardness, uniformity, and thickness control of spinning different compositions of PDMS films.
3. The experimental characterization of using the DISCO Backgrinder, DAG810, for the processing of wafers with PDMS elastomer superstrates.
4. The experimental characterization of spinning and curing thick, planar layers of PDMS on wafers.
5. Documenting the process used to keep the backside of wafers clean post-PDMS spin.
6. An SOP and the experimental characterization for *molding* extremely thick layers of PDMS on top of wafers and wafer pieces.
7. Experimental results and conclusions for ultra-precise, extreme thinning of silicon wafers.
8. Documentation on the deposition conditions of thick polycrystalline germanium using low pressure chemical vapor deposition (LPCVD) and its surface roughness.



## 2 Process development and experimentation

### 2.1 Process flow

The process for quickly and reliably manufacturing nano- and micro-structures embedded within flexible materials is depicted in Fig. 1. Note that the intended purpose of the embedded structures of this process is to build optical metasurfaces, which require low loss across a wide range of incident wavelengths of light. PDMS is a suitable elastomer for this intended purpose, which is why it has a rich history of use in optics research. It is also a bio-compatible material, making it suitable for biomedical applications. However, the process depicted in Fig. 1 can be used with any flexible material that can be spun or molded thickly and uniformly on top of the structures after they are patterned on the handle material stack.

The proposed process flow, illustrated in Fig. 1, is different from the conventional manufacturing process because it employs a wafer backgrinder to remove most of the handle wafer, instead of relying solely on a wet etch process to release the embedded structures. We begin by depositing a relatively thick ( $3\mu\text{m}$ ) layer of germanium via chemical vapor deposition (CVD) on top of a silicon wafer with a 300nm oxide layer. The deposition of germanium is completed using ThermcoPoly1, and the oxide growth is completed using Thermco1. Although the germanium layer is conventionally used as a sacrificial layer during a wet etch process to release the embedded microstructures at the end of the process, in this process it is instead used as a mechanical buffer layer between the silicon handle wafer and the silicon structure layer. We use an oxide layer that functions as an etch stop during the P5000 dry etching process of the silicon microstructures, preventing the grooves of the structures from becoming too deep, and thus removing the risk of PDMS seeping into the handle wafer material.

The step of embedding the structures in the flexible material after patterning using the dry etching process, depicted in Fig. 1 (d), is re-imagined for this process. Conventionally, the liquid PDMS mixture, before it is cured, is deposited on and in-between the microstructures by spinning. In our experiments, as presented in Section 2.8, it was determined that it is impossible to spin the hard-curing, low-viscosity formulation of PDMS that our process necessitates to be hundreds to thousands of nanometers thick. This thickness is both beneficial for the manufacturing process, as it is much less fragile and easy to handle than the hundred nanometer thick conventionally manufactured counterpart, and this added thickness may also be exploited for refractive optical purposes. Thus, we developed a molding process, as detailed in Section 2.9, to achieve thick, relatively incompressible, and uniform layers of cured PDMS.

The process steps depicted in Fig. 1 (e)-(f) release the embedded structures from the handle materials. The conventional manufacturing process achieves this through the wet etch of the germanium layer. This takes around a week of time to complete for a 4" wafer due to the minuscule area of the periphery of the germanium layer that is exposed to the etchant. To drastically decrease the processing time, we mechanically grind away the handle wafer materials, stopping within the protective germanium layer, thus exposing its entire surface area from the bottom. From our experimental results, the DISCO backgrinder, DAG810, has the precision and accuracy to consistently stop within  $2\mu\text{m}$  of the intended thickness target, thus allowing it to stop grinding

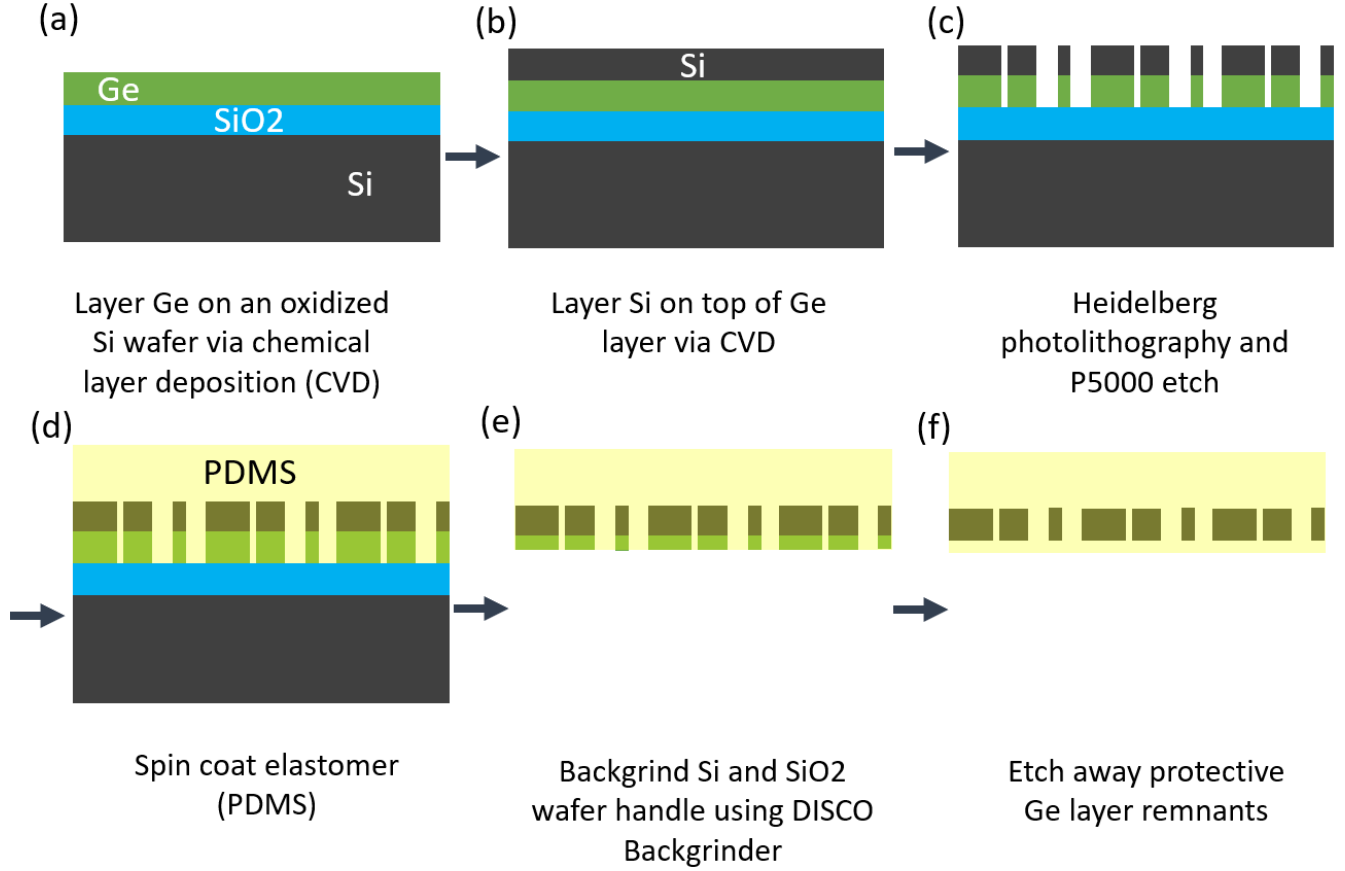


Figure 1: Schematic of the complete process flow proposed to quickly and robustly manufacture micro- and nano-structures embedded in flexible materials. Steps (a)-(d) of the process are the same as those used to conventionally create elastomer-embedded microstructures. The main difference is that instead of using the germanium layer as a sacrificial layer for the wet chemical etch release of the elastomer, it is instead used as a protective layer for the mechanical removal of the handle material stack using a wafer backgrinder, in step (e). This exposes a large area of germanium, making etching very quick in step (f).

within the  $3\mu\text{m}$  protective layer of germanium. Afterwards, due to the now large exposed area of germanium, it can be removed using a wet etch process in a negligible amount of time.

The final product of this process is patterned microstructures within a flexible material. Whereas the conventional manufacturing method can take on the order of a week to complete, the proposed process can be theoretically completed within an hour, using a well-characterized process tool in SNF.

## 2.2 Wafer piece backgrinding

The SNF community is lacking both an SOP describing the processing of silicon pieces using the DISCO wafer backgrinder, DAG810, as well as the experimental characterization of the accuracy of processing pieces. We sought to both document the feasibility of using the wafer backgrinder to process sample pieces in the development of our embedded microstructure manufacturing process.

As depicted in Fig. 2, we developed a process for precise wafer piece thinning, with uniform height control. For maximal utility for experiments related to the development of an embedded microstructure manufacturing process, we aimed to develop a piece backgrinding technique that exhibited the following characteristics:

1. Does not use etching chemicals that are not selective to PDMS.
2. Does not require heat in excess of  $150^{\circ}\text{C}$ , to prevent the disintegration (i.e., burning) of the PDMS.
3. Achieves thickness variation across a single pieces of less than  $3\mu\text{m}$ , in order to be able to stop within the  $3\mu\text{m}$ -thick protective layer of germanium.
4. Preferably exhibits consistent thickness uniformity across multiple pieces bonded to a single handle wafer, allowing for the parallel processing of pieces in the backgrinder at the same time.

As suggested by the DISCO Backgrinder DAG810 tool owner, Saeed Nejad, we elected to use jeweler's wax to bond the wafer pieces to the 4" handle wafer. To validate that the height control of bonded pieces is adequate, we cleaved three pieces of identical dimensions ( $25\text{mm} \times 20\text{mm}$ ), and prepared jeweler's wax for each of them that was equal in mass to 4 decimal places ( $0.0470\text{g}$ ), as depicted in Fig. 2 (a). Next, the three equally-weighted piles of wax were melted on the handle wafer using a hot plate set to  $110^{\circ}\text{C}$ . The cleaved silicon pieces were then placed on the melted wax puddles, and pressed down using an aluminum block, as depicted in Fig. 2 (b). After precisely 1 minute of heating and applying equal pressure to the pieces using the aluminum block, the heat from the hotplate was turned off, allowing the wax to harden, thereby bonding the pieces to the handle wafer, as depicted in Fig. 2 (c). Releasing the pieces from the handle wafer then simply requires reheating the handle wafer to  $110^{\circ}\text{C}$ .

Although this piece bonding and debonding process did not damage the PDMS superstrate, the thickness uniformity was unsatisfactory, as depicted in Fig. 3. A handle wafer is chosen with a

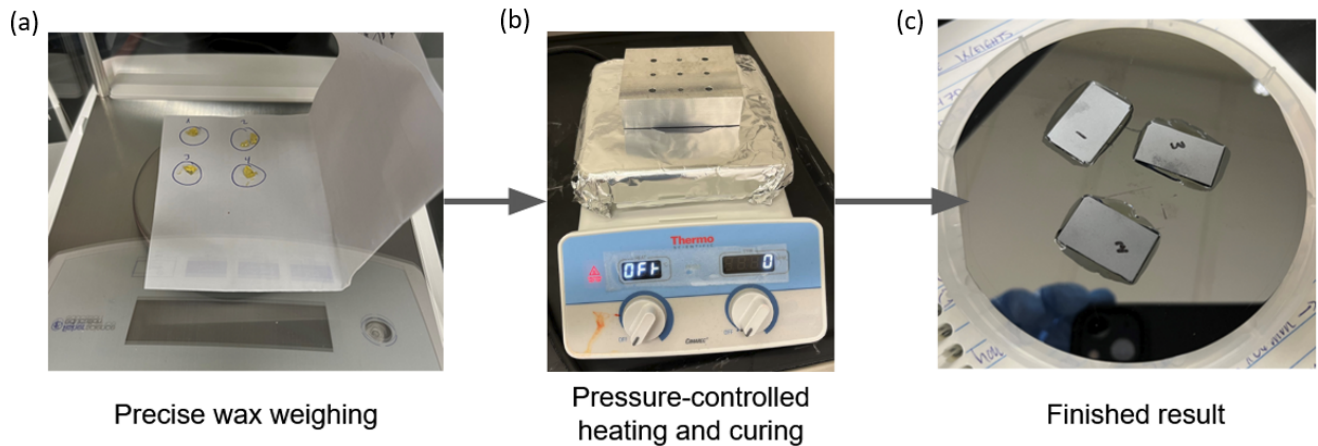


Figure 2: Process devised for the precise bonding of silicon pieces to a silicon handle wafer using jeweler's wax.

variation in height of  $1\mu\text{m}$  across the entire 4" wafer, as depicted in Fig. 3 (a), as measured using a Mitutoyo height difference-measuring drop gauge. The cleaved silicon pieces, which measured 25mm in length, exhibited a variation of at most  $2\mu\text{m}$  in height across, as depicted in Fig. 3. After the bonding process illustrated in Fig. 2, the measured thickness variation across a single piece was of around  $10\mu\text{m}$ , as depicted in Fig. 3. Although this process is highly precise, the nanostructure embedding process requires micron-level precision due to limitations in the height of the germanium deposition. Therefore, further experiments with the backgrinder used complete wafers.

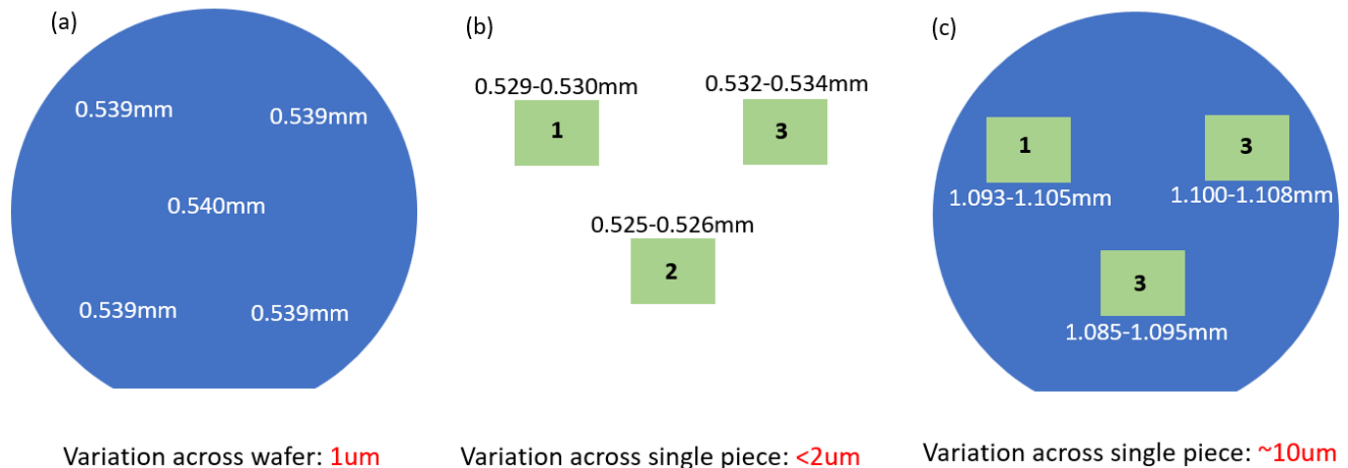


Figure 3: Height uniformity results of bonding silicon pieces to a handle wafer using jeweler's wax.

## 2.3 Material growth

As indicated in Fig. 1, the process employs three material growth steps: 1. Grow about 300nm of  $\text{SiO}_2$  on a silicon wafer. 2. Grow  $3\mu\text{m}$  of germanium 3. Grow  $1\mu\text{m}$  of polycrystalline silicon (poly-Si). These steps are described below:

1. **Oxide Growth:** The thermal oxide growth is standard and consistent. We used the clean furnace tool, thermco1, for growing 300 nm of thermal oxide. We ran the *wetox* recipe under a temperature of  $1050^\circ\text{C}$  for 25 minutes for 25 wafers. Using elipsometry, we determined that the oxide thickness across 25 wafers is  $299\text{nm} \pm 1\text{nm}$ , as shown in Fig. 4

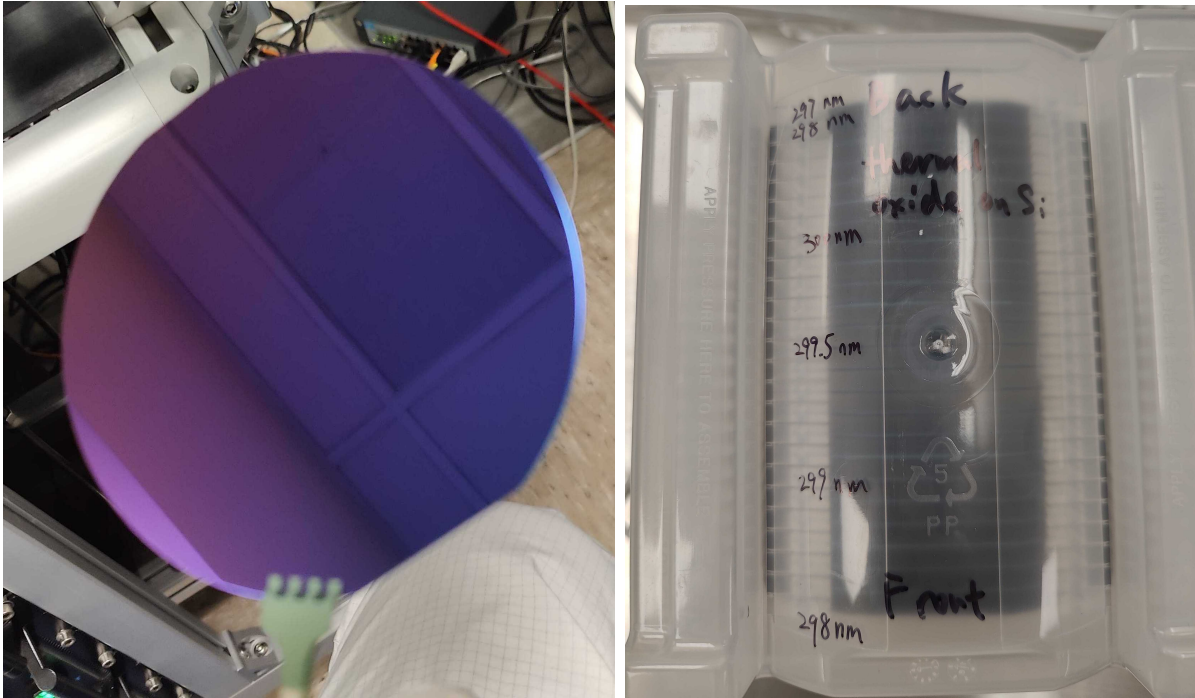


Figure 4: Left: Oxidized Silicon wafer. Right: Oxide thickness across 25 wafers.

2. **Germanium Growth:** For all the germanium and poly-Si deposition mentioned in this subsection, we selected a gas flow rate of 300 sccm, which is the center value of the recommended range of 200 sccm to 400 sccm.

We first tried directly growing germanium on oxide, and similarly on silicon with its native oxide, under  $450^\circ\text{C}$  for two hours, but germanium nucleates poorly on oxide surfaces. It resulted in non-uniform film deposition as shown in Fig. 5.

The solution is to grow a thin layer of poly-Si first, as provided conveniently in the recipe *PGE*. The poly-Si layer has good compatibility with both the oxide beneath and the germanium above. To determine the germanium growth rates of both the poly-Si and germanium,

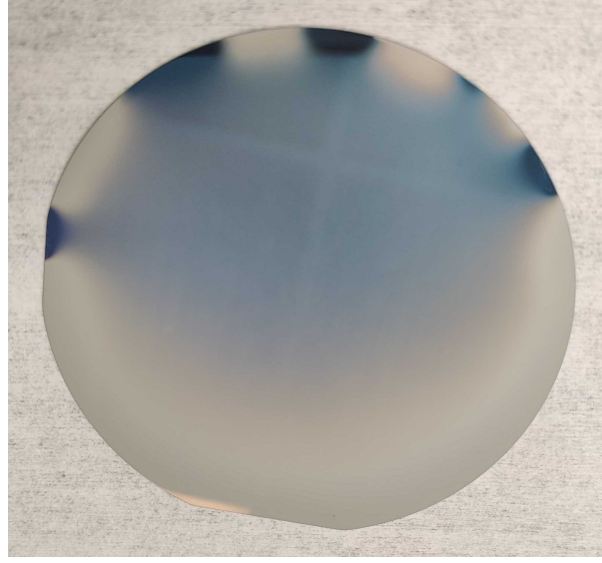


Figure 5: Run 1: Non-uniform germanium deposition when directly grown on Oxide.

we first deposited poly-Si for 30 minutes under  $625^{\circ}\text{C}$ , followed by 2 hours of germanium deposition under  $400^{\circ}\text{C}$ . The SEM image of the cross-section is shown in Fig. 6.

The results of the growth characterization trial are acceptable, with uniform deposition and a surface smoothness of 100 nm. The surface roughness could be further decreased by lowering the germanium deposition temperature, but we proceeded without further optimization due to a limited time and budget. We calculated the germanium growth rate to be  $9.17\text{nm}/\text{min}$  and the poly-Si growth rate to be  $9.67\text{nm}/\text{min}$ .

We proceeded for the  $3\mu\text{m}$  germanium growth with the same temperature of  $400^{\circ}\text{C}$ . We first deposit poly-Si for 5 minutes, then germanium for 5 hours and 30 minutes. Lastly, we deposited the  $1\mu\text{m}$  poly-Si device layer by running the P620POLY process for 1 hour and 30 minutes. With  $3\mu\text{m}$  thickness, the surface roughness is no longer sufficiently low enough to resolve sharp details in reflections from the surface. As demonstrated in Fig. 7, only a dull reflection of light sources are visible in the reflection from the surface. The cross-section SEM is shown in Fig. 7.



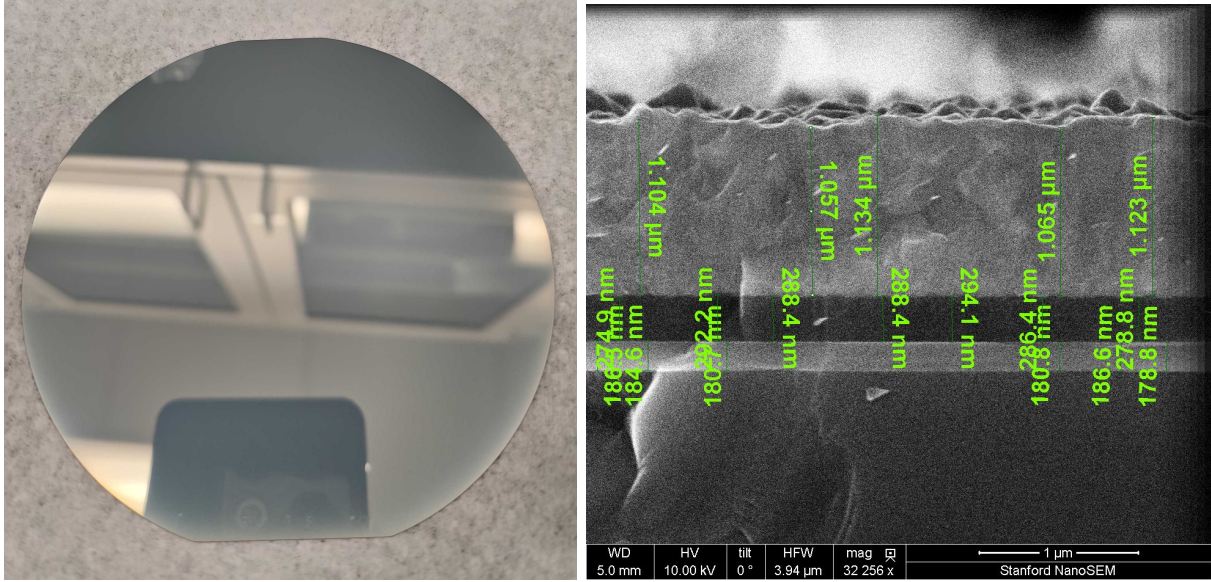


Figure 6: Run 2: **Left**:  $1.1\mu\text{m}$  germanium layer with 100 nm of surface smoothness. **Right**: SEM image of cross-section. The materials from bottom to top are: bulk silicon, oxide, poly-silicon, and germanium.

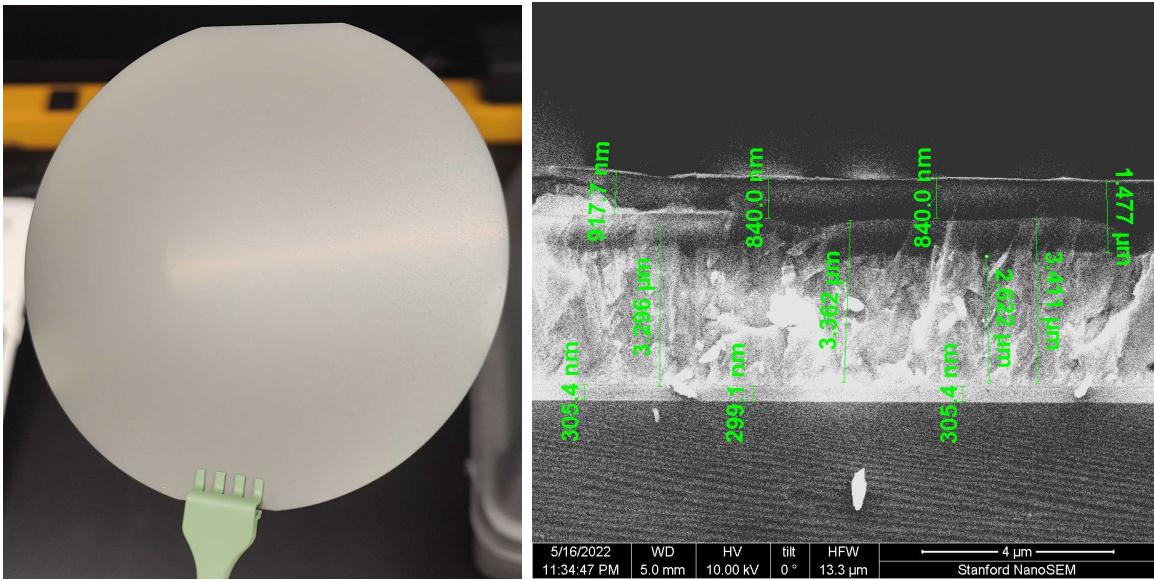


Figure 7: Run 3: **Left**: optical reflection of  $3\mu\text{m}$  of germanium and  $1\mu\text{m}$  of poly-Si. **Right**: SEM image of the cross-section. The materials, from bottom to top, are: bulk silicon, oxide, poly-Si (very thin, cannot be resolved here), germanium, and poly-Si.

## 2.4 Microstructure patterning

As our ultimate goal is to fabricate curved metasurfaces, which are ultimately arrays of microstructures, we fabricate such structures for this project in order to determine the feasibility of fabricating microstructures on rough surfaces and to determine the degree to which they can be embedded into the elastomer. Our target trial pattern is shown in Figure 8. It consists of stripes with varying widths, ranging from  $1\mu\text{m}$  to  $5\mu\text{m}$ .

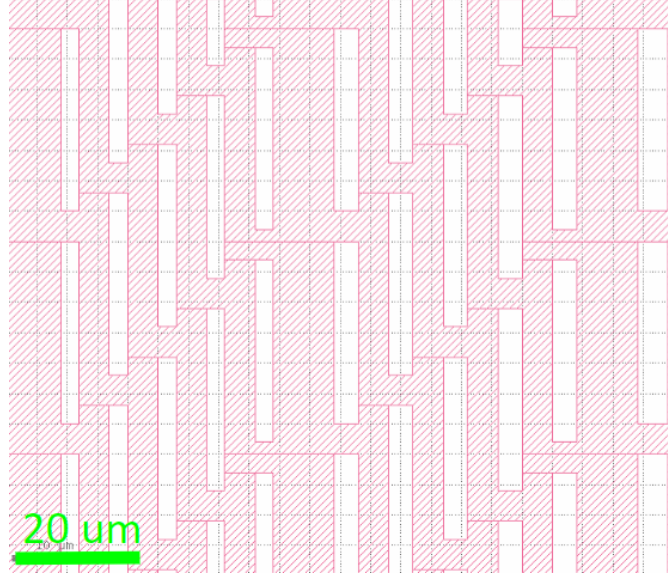


Figure 8: Target trial pattern for the photolithography process.

Although the final microstructures are fabricated on the material stack detailed in Section 2.3, we first perform the same patterning process on a polished silicon wafer to provide a reference. We first spin coat  $1\mu\text{m}$ -thick SPR3612 photoresist on the silicon wafer. We perform a dosage sweep to determine the optimal value of the Heidelberg photolithography process for our use case. We sweep the dosage parameter from  $40\text{ mJ}/\text{cm}^2$  to  $70\text{ mJ}/\text{cm}^2$ . The patterning results after development under a microscope are shown in Fig. 9. We can observe that under a dosage of  $40\text{ mJ}/\text{cm}^2$ , the photoresist is not fully removed after development, indicating that the dosage is insufficient. Under the dosage of  $60\text{ mJ}/\text{cm}^2$  and  $70\text{ mJ}/\text{cm}^2$ , the neighboring stripes become connected, indicating that the dosage is too large. Under a dosage of  $50\text{ mJ}/\text{cm}^2$ , the pattern is closest to our target. We select  $50\text{ mJ}/\text{cm}^2$  as the best exposure dosage for our target pattern on a polished silicon surface. We also sweep the defocus parameter to determine the optimal value for our process. The result shows that the patterning is less sensitive to defocus. We select the default setting on the Heidelberg machine,  $-2$ , for our process.

However, things become different when performing photolithography on a rough surface. The variation of the rough surface is on the order of  $100\text{nm}$ , which is close to the wavelength of the ultra-violet light used for exposure. The light could interact with the spots and suffer from scattering.



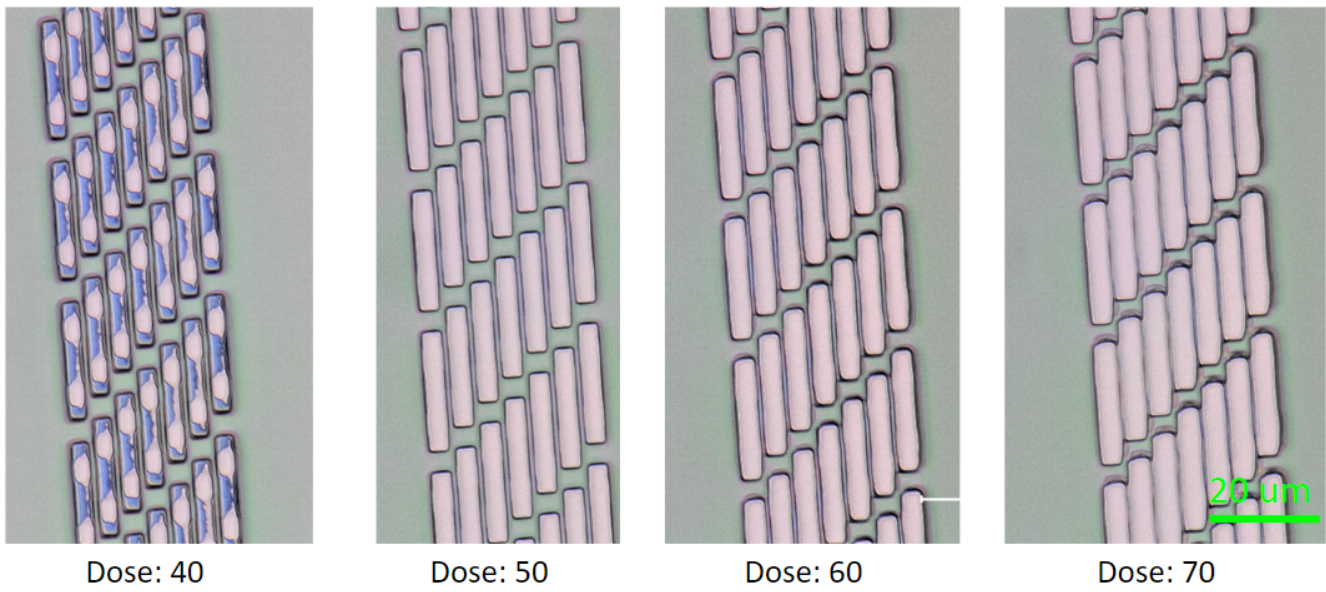


Figure 9: Patterning dosage test results on a smooth surface in the photolithography process.

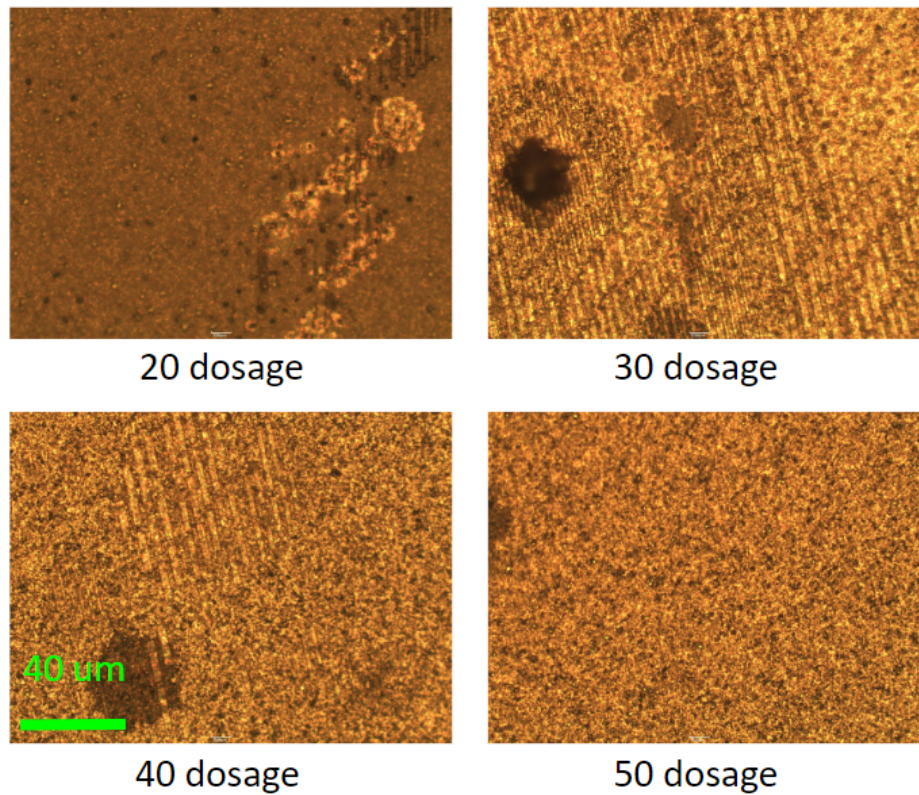


Figure 10: Patterning dosage test results on a rough surface in the photolithography process.

The surface roughness thus affects the optimal dosage of the patterning process. We perform a dosage test on the rough surface similar to the one described above. We sweep the dosage from 20 mJ/cm<sup>2</sup> to 50 mJ/cm<sup>2</sup>. The patterning results after development under a microscope are shown in Fig. 10. Under a dosage of 20 mJ/cm<sup>2</sup>, the photoresist is not removed after development, indicating that the dosage is insufficient. Using 50 mJ/cm<sup>2</sup>, the pattern is still not visible, indicating that the dosage is too large. Under a dosage of 30mJ/cm<sup>2</sup>/40mJ/cm<sup>2</sup>, we can see our target rectangular stripes appear on the surface. Thus, 30mJ/cm<sup>2</sup>/40mJ/cm<sup>2</sup> is the optimal exposure dosage for the target pattern on the material stack described in Section 2.3.

## 2.5 Etching and PDMS filling

After writing the test patterns using Heidelberg photolithography, we dry-etched the test patterns using lampoly. The etch consists of a break-through step with  $C_2F_6$  for 10 seconds, then a main etch with  $Cl_2$  and  $HBr$ , and finally an over-etch step with  $HBr$ . The time ratio of main etch to over-etch is kept as 1:4 for best sidewall quality, and the total calculated time is 227 seconds for an etch rate of 4.4nm/s. For testing, we picked three total etch times: 200s, 250s and 300s. The etched results are shown in Fig. 11. The etched test pattern is clearly visible, but the germanium layer is not etched through and there is not much difference between the tested values of etching time. A possible explanation is that the chamber chemistry changes once germanium is exposed.

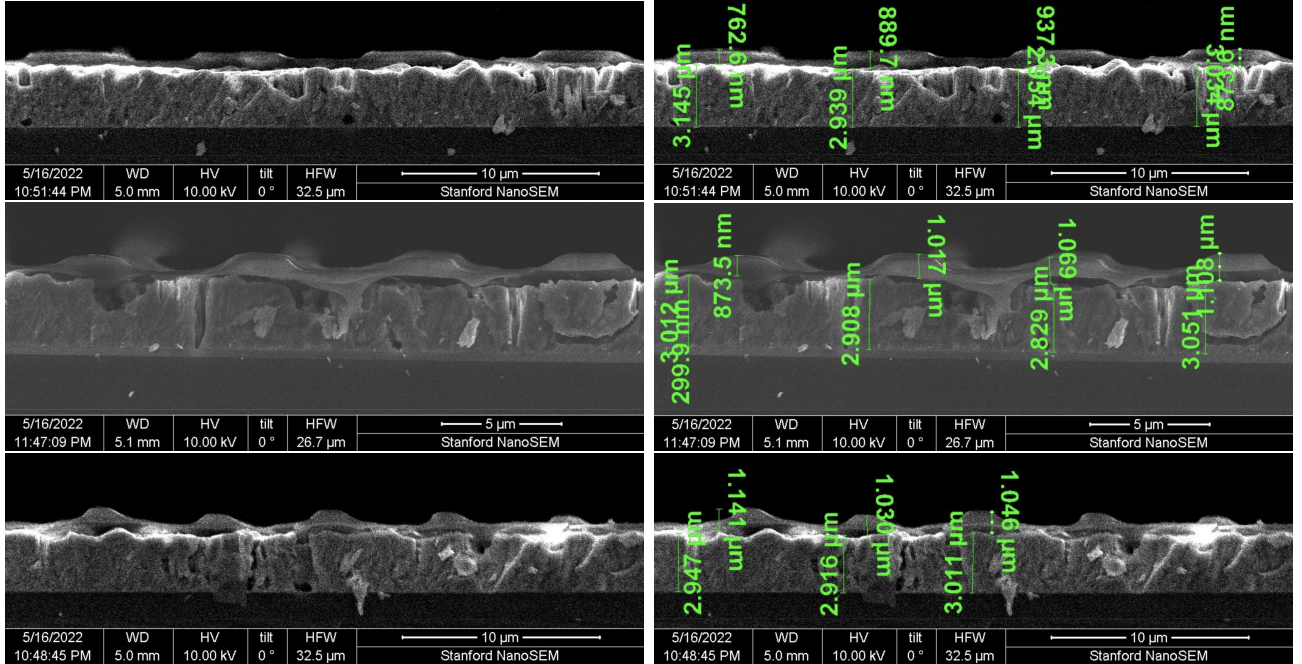


Figure 11: Exemplary regions from etch 1, 2, and 3, with visible Si test-pattern structures, but without germanium etched through, as had been expected.

As seen from the SEM image, the test pattern sidewall is not vertical, which could be due to the mask not being selective enough. This could be improved in the future by replacing the



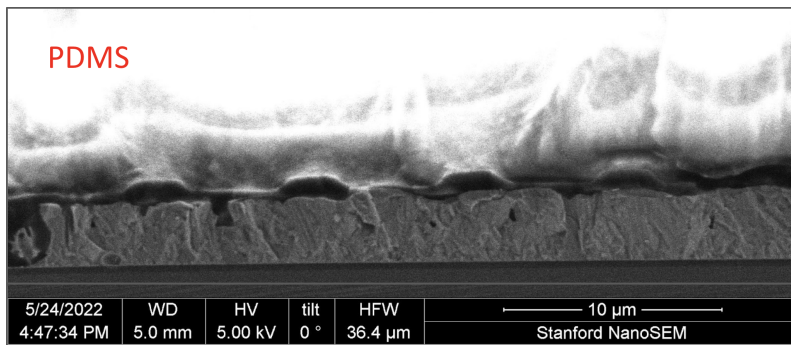


Figure 12: The filling of test patterns with PDMS.

photoresist with harder alternatives, or by using other patterning methods, like liftoff. For this project, these etching results are satisfactory.

We then spun PDMS on top of the etched devices to test its filling properties with the test pattern. Since our test patterns have spacing of several microns, the filling is without issues, as shown in the cross-section SEM image in 12. The image quality is affected by charging of the PDMS, but the adequate filling of the device features is still evident.

## 2.6 PDMS formulation

As described in Section 2.1, polydimethylsiloxane (PDMS), specifically SYLGARD 184, was chosen as the flexible embedding material for this study. This is due to its favorable optical properties that led to its widely-documented success as a flexible optical material in academic research. PDMS is a polymer that consists of a molecular structure containing both carbon and silicon. PDMS monomers cross-link during the curing process, which is facilitated by the curing agent upon the application of heat to a mixture of SYLGARD 184 base and curing agent. The PDMS characteristics of interest are the fluid viscosity, for adequate groove penetration, and stiffness of the cured elastomer. These are dependent on the PDMS formulation and curing parameters, namely the ratio of SYLGARD 184 base to curing agent and the curing temperature and time.

The effect of PDMS curing temperature and time is well-documented. [1] The relationship between curing temperature and curing time has an exponentially decreasing relationship to meet the curing condition (the point at which PDMS is fully cured). For example, it takes 2 days for PDMS to fully cure at room temperature, 45 minutes at 100°C, and 10 minutes at 150°C. Furthermore, it is well-documented that PDMS cures with a higher Young’s modulus (meaning that it is more stiff) with higher curing temperature, as the higher energy input into the system results in more crosslinks being produced in the polymer network of monomers. [1] Thus, for our process, which requires an elastomer with high stiffness to ensure compatibility with the wafer backgrinder processing, it is beneficial to cure the PDMS at a relatively high temperature for long periods of time.

The relationship between the SYLGARD 184 base and curing agent of the PDMS formulation is not well documented in the literature, as it ranges from highly plastic formulations (with upwards

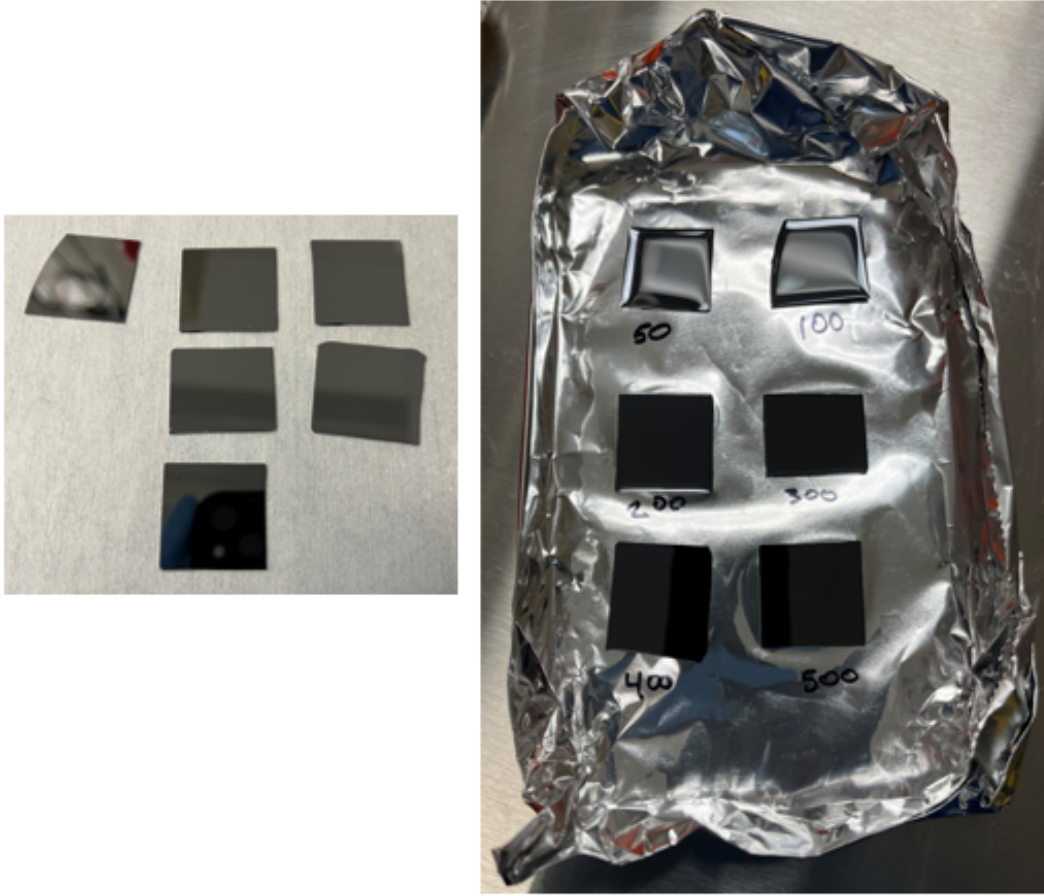


Figure 13: Figure depicting the experimental setup of the silicon pieces used to characterize the hardness of PDMS for different base to curing agent formulations. (Left) The pieces were cleaved to all be  $25\text{mm} \times 25\text{mm}$ . (Right) After spinning, the samples were all baked at the same time, in the same aluminum foil boat, to ensure that conditions are the same.

of 20 parts base to 1 part curing agent), down to the standard formulation of 10:1, down to only 3:1. We sought to characterize formulations of PDMS with values of Young's modulus that are higher than those presented in the literature as a direct result of the base to curing agent ratio. These experiments were performed using  $25\text{mm} \times 25\text{mm}$  pieces of silicon wafers. The samples are shown in Fig. 13, and the results of the curing experimentation are depicted in Fig. 19.

The results of the curing experimentation of the different formulations of the PDMS, presented in Fig. 19, were measured using a film thickness measurement and compression technique developed specifically for this project, as depicted in Appendix 5.3. From the experiments, it is determined that there is a steady increase in the stiffness of the cured PDMS film as the amount of curing agent in relation to the amount of PDMS base is increased. However, there is a marked increase in observed stiffness from the 3:1 ratio formulation to 1:1 ratio one. Another marked increase of

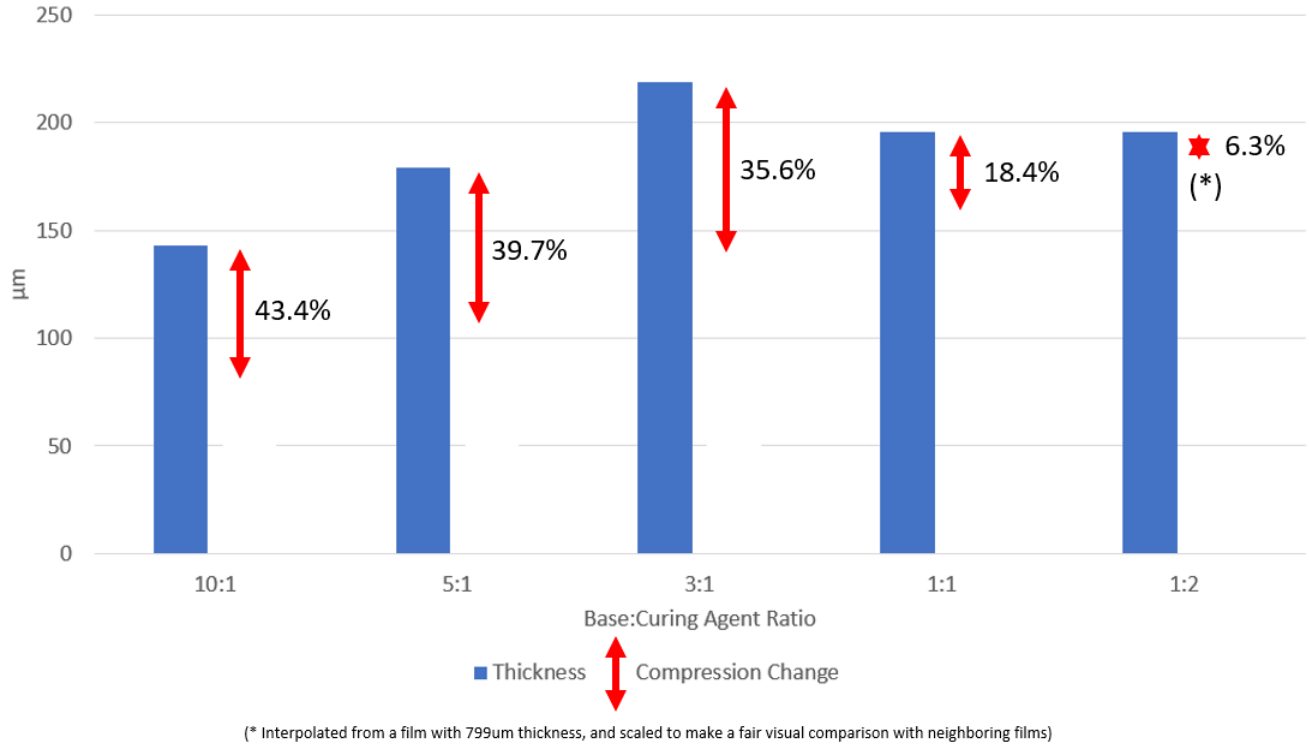


Figure 14: PDMS Compression experiment results. A steady increase in stiffness is observed as the amount of curing agent is increased. Drastic increases are observed for both 1:1 and 1:2 ratio formulations of PDMS. 1:2 ratio was measured using a film with a thickness of 799μm (achieved using molding, as described in Section 2.9) and linearly interpolated down to be plotted here. This is because a 1:2 ratio PDMS film could not be spun thicker than 25μm due to the water-like viscosity of the base-curing agent mixture at this ratio.

stiffness is again observed from 1:1 to 1:2 ratio formulation PDMS.

For our proposed process, there are two benefits to choosing a PDMS formulation with higher amounts of curing agent than conventionally used. The first is that it results in stiffer PDMS films, which allows the backgrinder to apply pressure to the sample without significant compression. The second, more subtle reason, is that the SYLGARD 184 base-curing agent solution is much less viscous, with a consistency similar to that of water for 1:2 ratio formulation (as opposed to a honey-like consistency for 10:1 ratio formulation PDMS). This is desirable, as it allows the solution to seep into the grooves of the patterned microstructures without the use of a viscosity-reducing dilutant, such as toluene. We chose to move forward with the 1:2 ratio formulation of PDMS due to these desirable properties. Further dilution of the PDMS solution with curing agent was deemed unfeasible for an experimental process with a tight budget, as the commercially available PDMS kits are available with containers that hold 10 parts of base to 1 part of curing agent.

## 2.7 Precise wafer backgrinding

The backgrinder operates by removing material using a rotating grinding wheel that moves downwards, towards a sample that is attached to a rotating chuck with a vacuum seal. An overhead depiction of the working mechanism of the backgrinder is depicted in Fig. 15. The center of rotation of the grinding wheel is offset from that of the vacuum chuck, but by virtue of the rotating chuck, the rotation of the grinding wheel evenly removes material from across the entire surface of the sample. The machine operator has control over all operating conditions, the most important of which are the spindle spin speed, chuck spin speed, and spindle z axis movement speed. Each of these parameters affects the quality, precision, sample heating, and grinding force during the thinning process.

Our sample, composed of the elastomer-embedded structures on top of the handle material stack, is placed with the elastomer downwards, on the vacuum chuck, such that the handle materials can be removed. The grinding must be done as delicately as possible in order to not shatter the thin material being removed on top of the soft elastomer. Without a straightforward way to measure the forces exerted on the sample by the spindle as a function of the operation variables, we consulted the literature to find the optimal parameters for our process. Although, as we established in Section 2.6, we selected a formulation of PDMS that exhibits a miniscule compression, of only 6.3%, when compared to more conventional formulations, this is still a non-trivial amount, as samples that are typically processed by the backgrinder are rigid. Processing compressible samples thus poses parameter selection challenges that are not typically encountered for wafer backgrinding. The parameters must be carefully tuned to prevent excessive cantilever forces that arise from the off-centered spindle applying pressure on one side of the sample with a compressible superstrate.

Prior studies have established that the most gentle grinding process (i.e., that which exerts the least amount of force on the sample) use lower spindle and chuck spin speeds, as well as lower feed rates. [5] However, too low of a feed rate for given spindle and chuck spin speeds would result in friction heating of the material without it being removed sufficiently quickly enough to prevent damage. Thus, experimentation and fine-tuning is required to determine the set of parameters that best process our flexible superstrate material stack. The promising results of these experiments

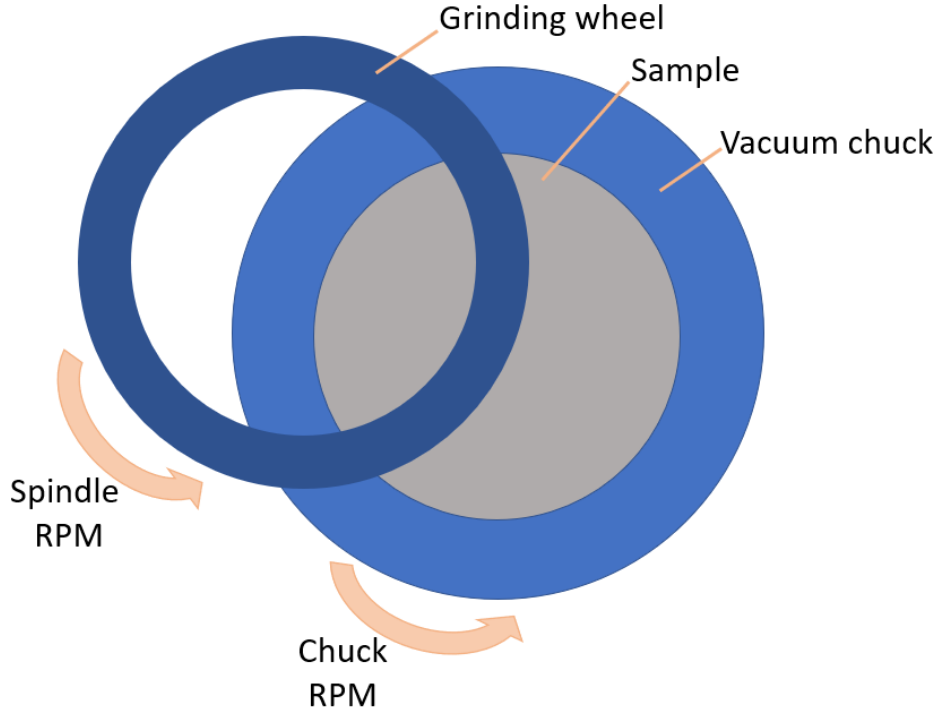


Figure 15: Overhead schematic of the working principle of the wafer backgrinder.

are provided in Sections 2.8 and 2.9, and the final selected parameters for the spinning process are provided in Appendix 5.2.

## 2.8 Spin-coating PDMS

The conventional method of depositing PDMS onto a handle material stack is through spinning. This typically works well for most experimental applications, as these use the more viscous 10:1 PDMS formulation, resulting in thicker films than those achievable with the less viscous 1 (base) : 2 (curing agent) ratio PDMS formulation selected for our process 2.6. Despite the viscosity of the 1:2 ratio PDMS being similar to that of water, liquid beading on the wafer was still visible along the edges due to the surface tension that was manifesting itself between the perimeter of the wafer and the liquid PDMS. Thus, there exists a lower limit on the minimum acceptable spin speed of the coater, such that an adequately uniform layer of cured PDMS is achieved.

For a 1:2 ratio formulation of PDMS, the thickest layer we were able to achieve through spinning, with a variation of at most  $2\mu\text{m}$  across the entirety of a 4" wafer, was of  $24\mu\text{m}$ , as depicted in Fig. 16. To help facilitate a clean spinning process, we made use of protective *blue sticky tape* on the backside of the wafer during spinning—a process that is documented in Appendix 5.1. To determine the accuracy of the backgrinding process for a sample with a PDMS superstrate, we tested by grinding  $50\mu\text{m}$  of material using the recipe specified in Appendix 5.2. Expecting the sample depicted in Fig. 16 to be thinned from a height of  $569\mu\text{m}$  to  $519\mu\text{m}$ , it instead reached a height of  $517\mu\text{m}$ , stopping within  $2\mu\text{m}$  of the specified target. This is satisfactory, as it falls within



Figure 16: Schematic of the material stack for grinding with a PDMS superstrate.

the  $3\mu\text{m}$  germanium buffer limit of our process. However, when trying to continue grinding to a height of  $24\mu\text{m}$  (down to the level of the PDMS layer), the backgrinder issued a *loaded workpiece too thin* error mid-grind after reaching a working height of  $107\mu\text{m}$ . Subsequent attempts to restart grinding resulted in alternating errors of *loaded workpiece too thin* and *loaded workpiece too thick*. Thus, we determined that the working height of the backgrinder must be at least  $110\mu\text{m}$  in order for it to perform reliably.

Given our inability to spin very thick layers of our preferred 1:2 ratio PDMS, we attempted to complete the backgrinding process using the more conventional 10:1 ratio PDMS, for which there exist developed processes for thick and uniform spinning. The more conventional process calls for spinning very thick, initially uneven 10:1 ratio PDMS, and letting it to cure at room temperature on a levelled surface over the course of 24 hours. It thereby undergoes the opposing but complementary processes of gravity-induced reflow and polymerization at room temperature. Post-room temperature reflow, the sample is baked at  $110^\circ\text{C}$  to complete curing of the PDMS. This process is described by Fig. 17. After 24 hours of reflow, the process yielded a  $165\mu\text{m}$  thick layer of PDMS with a maximum non-uniformity of  $15\mu\text{m}$  across the 4" wafer, with the maximal difference occurring between an edge and the center of the sample due to the initial beading of the liquid PDMS (as opposed to the perhaps more expected outcome of the maximal height difference occurring between maximally distant edges of the 4" wafer). Although this sample is acceptable for the purpose of probing the backgrinder's ability to thin away the entire silicon wafer substrate, the literature reports that micron-level uniformity is possible with 72 hours of reflow. [3]

Thinning the silicon handle of the reflowed sample completely away is unsuccessful, as shown in Fig. 18. The vacuum seal of the chuck failed at a working height of approximately  $250\mu\text{m}$  (when there was about  $85\mu\text{m}$  of silicon material left to be removed), forcing an emergency stop of the grinding process. The suspected cause of failure is due to the uneven pressure exerted on the surface of the sample by the grinding wheel during the material removal process, as described in Section 2.7. When the silicon reached a height of  $85\mu\text{m}$ , it was incapable of withstanding the simultaneous cantilever and rotational forces exerted by the grinding wheel, causing material failure. The conclusion of this experiment is that, for PDMS layers in excess of  $110\mu\text{m}$ , which is necessary for the operation of the DISCO DAG810 to operate, a more stiff, but still flexible,



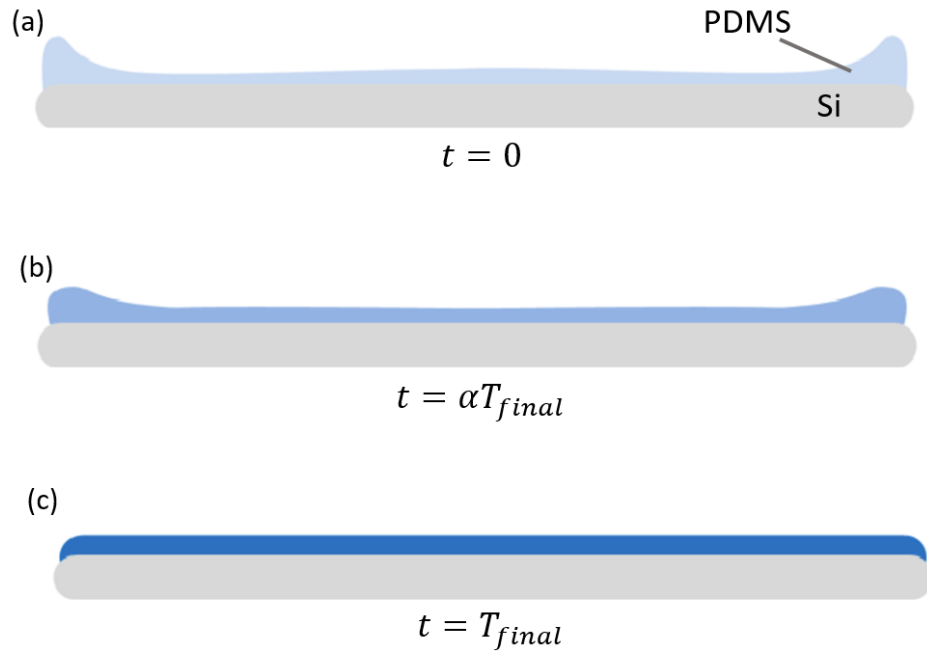


Figure 17: The reflow-polymerization process. (a) Immediately after spinning, at  $t = 0$ , excessive edge beading is present. (b) As time progresses, the PDMS begins to polymerize, but it is simultaneously reflowing due to the force of gravity and surface tension that is pulling it flat. (c) After 24-72 hours of the reflow-polymerization process at room temperature, the PDMS is uniform to within microns across the entire 4'' wafer. This figure is adapted from [3] with permission from *L'archive ouverte pluridisciplinaire HAL* due to Creative Commons licensing.

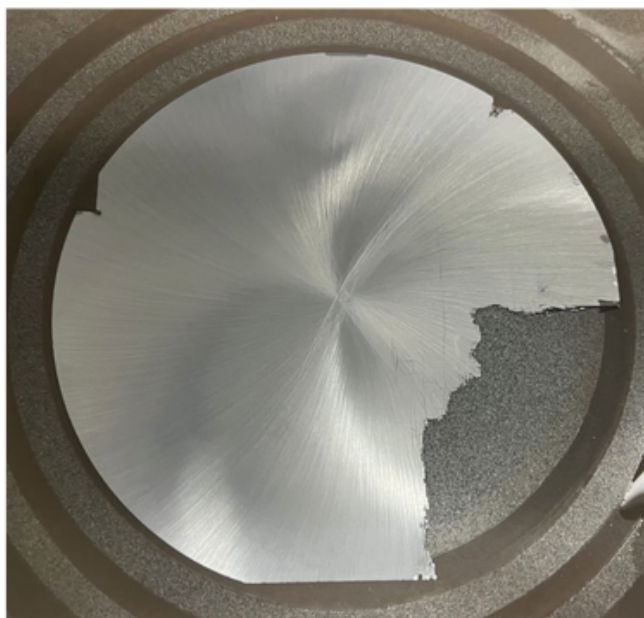


Figure 18: Grinding failure with thick 10:1 PDMS, caused by cantilever forces suffered by the sample due to uneven pressure exerted on the sample by the grinding wheel.

material than the 10:1 ratio PDMS is required. This is addressed in Section 2.9, through the development of a thick PDMS molding process that results in an elastomer with a relatively high Young's modulus.

## 2.9 Molding PDMS

Necessitated by the failure of the DISCO DAG810 backgrinder to process samples with extremely thin or highly compressible PDMS superstrates, we developed a molding process to layer thick, highly stiff PDMS. A molding-like process is required because of the low viscosity of the less compressible PDMS formulations before curing. The requirements for such a mold, as illustrated in Fig. 19, include:

1. The mold's materials are capable of withstanding at least 150°C for 30 minutes, which is the duration of baking the PDMS during the curing process.
2. The mold's materials are compatible with PDMS.
3. The walls of the mold must form a watertight seal with the bottom in order to prevent the low-viscosity PDMS from leaking.
4. The edges of the mold are easily removable once the PDMS is cured.
5. The bottom portion of the mold is perfectly flat, such that PDMS does not seep underneath the wafer and for gravity to perfectly flatten the PDMS.

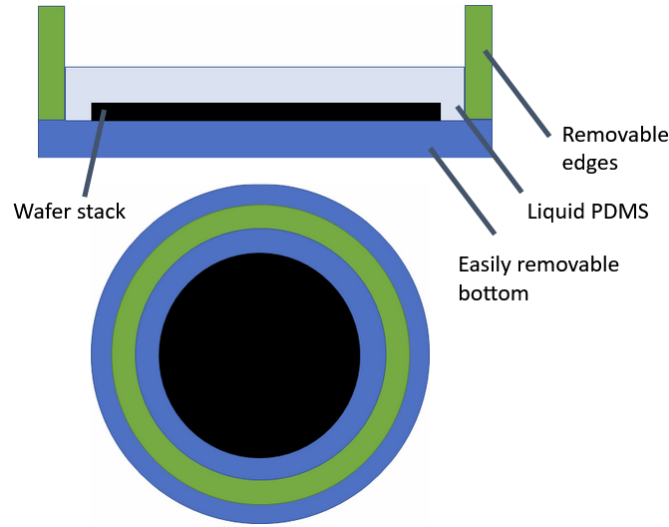


Figure 19: PDMS Mold Schematic, with a front view (Top) and the corresponding top-down view (Bottom)

6. The bottom can be easily separated from the sample once the PDMS cures.

As illustrated in Fig. 20, several trial molds were built before establishing a process that works well. Oven-curable polymer clay was chosen to fashion the walls of the mold. Polymer clay is an ideal prototyping material, because it is easily shapeable, can withstand high oven temperatures, it forms a watertight seal with glass and ceramics, it is easily removable, and it is highly compatible with PDMS, which is itself a polymer. Several candidate materials were tested for the bottom portion of the mold. Pyrex lab glassware was tested, as depicted in Fig. 20 (a). This option was ruled out because of a measured non-uniformity in height from the edge of the glassware to the center of  $740\mu\text{m}$ . This is due to the spinning manufacturing process used to make most glassware and cookingware, which does not have precise control of the height uniformity of the finished product. As illustrated in Fig. 20 (b), a  $0.125''$ -thick glass pane was tested, but failed due to warping of the glass under the high temperatures of the curing process. Finally, a flat ceramic tile was tested, as shown in Fig. 20 (c), which was satisfactory. The polymer clay was still soft at the end of the curing process, making it easily removable by hand. Curing was done on a hotplate levelled to  $\pm 0.1^\circ$  using a consumer self-calibrating digital leveller, the *Empire em105.9 9" Magnetic Digital Torpedo Level*, which is rated to be accurate to  $0.1^\circ$ . After trimming the edges of the cured PDMS using a scalpel blade, the blade was inserted horizontally in-between the ceramic tile and the wafer to create a slit. Dental floss was then used to remove the sample from the ceramic tile. Dental floss was the only cheap and widely available tool that is both flat and strong enough to remove the sample. Finally, the backside of the sample is scraped using the blade to remove any cured PDMS from the back.

The importance of using a perfectly levelled surface during the curing process is illustrated

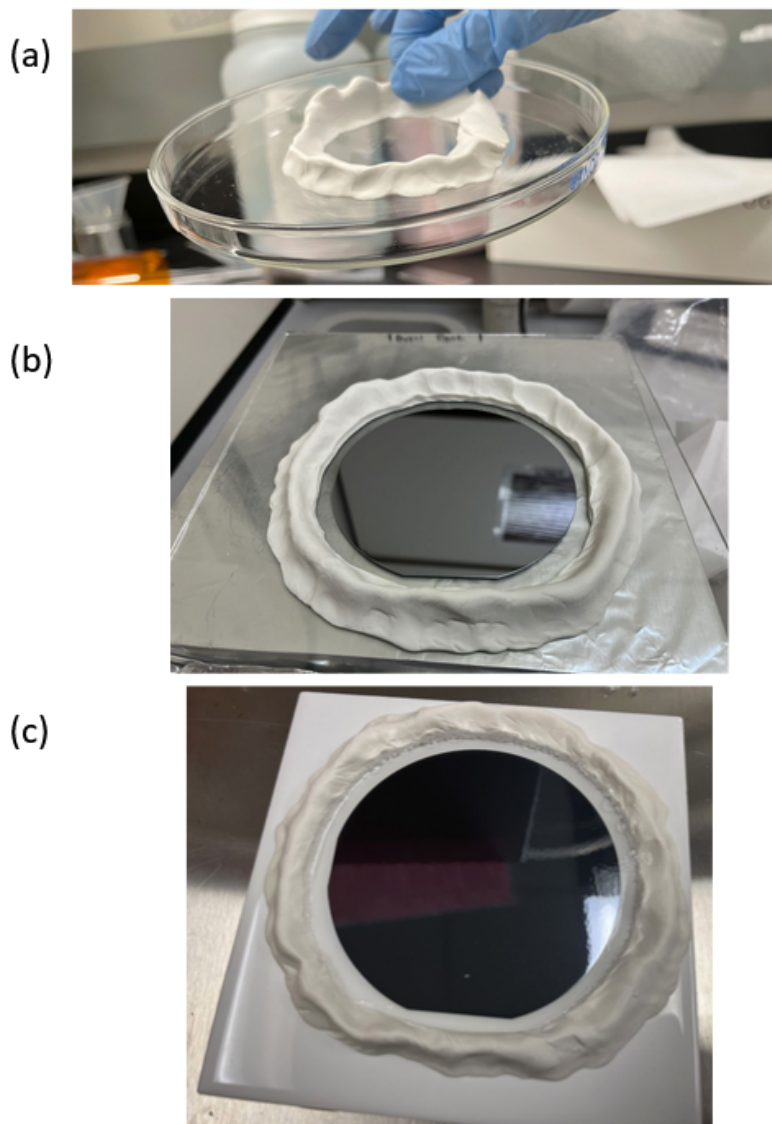


Figure 20: Images of the different trial molds. All three make use of polymer clay as the side walls. (a) Makes use of Pyrex lab glassware as the bottom, (b) makes use of a 0.125"-thick glass pane as the bottom, and (c) makes use of a flat ceramic tile for the bottom.

in Fig. 21, where the result of grinding is shown for a sample that was levelled to unit digit precision, resulting in edge-to-edge variation of  $475\mu\text{m}$ . The thinned side of the wafer succumbs due to uneven application of grinding forces before the grinding wheel even begins touching the opposing side of the wafer.

The result of the molding process with levelling to  $0.1^\circ$ , which yielded a film thickness of  $799\mu\text{m}$ , is depicted in Fig. 22. The surface of the PDMS is perfectly flat as a result of the molding process, which flows the PDMS over the edges of the wafer, thereby breaking the surface tension that would otherwise cause edge beading. However, the cured film is not parallel to the wafer surface: there is a maximal variation in height from one end of the wafer to the other of  $36\mu\text{m}$ . Within the  $5\text{mm} \times 5\text{mm}$  bounding area of the planned microstructure pattern, this amounts to a maximal variation of  $1.8\mu\text{m}$  in height. This is reasonable: if we consider that the consumer-grade digital level is precise to  $0.05$  degrees, simple trigonometry dictates that the height variation from one end of the  $100\text{mm}$  wafer to the other must be within  $87.2\mu\text{m}$ .

As visible in Fig. 22 (a), bubbles are also present at the edges of the PDMS cured using the levelled hotplate, which were not present when cured using an oven. This is likely due to the uneven heating of the sample from the bottom upwards, resulting in microscopic air bubbles created during the placement of the sample on the ceramic tile being released into the curing PDMS. This is an issue that can be ameliorated by placing the hotplate in a vacuum during the curing process. However, as the microstructure is in the middle of the sample, the bubbles do not interfere with the device.

The result from grinding the sample is depicted in Figs. 22 (b)-(c). Although the PDMS is compressible only by  $6.3\%$ , compared to the  $43.4\%$  compression rate of the  $10:1$  ratio PDMS tested in Section 2.8, this one was layered approximately 5 times thicker, resulting in cantilever forces of a similar magnitude. Although only  $187\mu\text{m}$  of silicon material were left to be removed, the sample did not break until the *spark-out procedure*, in which the sample is smoothed at the end by a spindle that is stationary in the  $z$  axis. The spark-out process produces high heat due to friction and high tensile forces due to the presence of protruding imperfections on the grinding surface prior to the start of the spark-out process. This violent process tore away both silicon and underlying PDMS, as shown in Figs. 22 (b)-(c), but it allowed for the careful removal of handle wafer material in the center of the sample, thereby exposing the underlying PDMS, as desired.

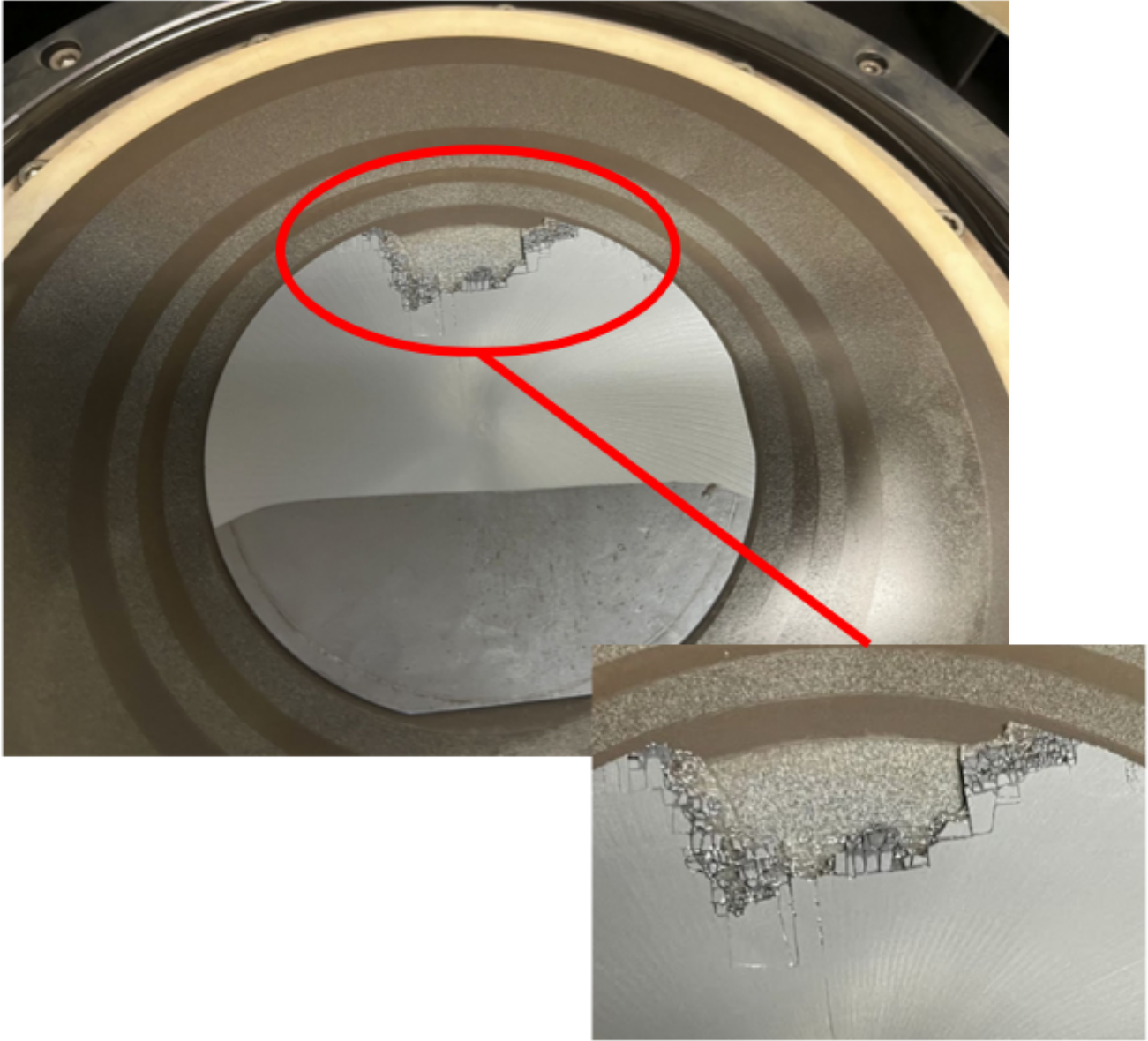


Figure 21: Grinding a wafer with unevenly cured PDMS across the surface results in premature chipping of the handle material stack.



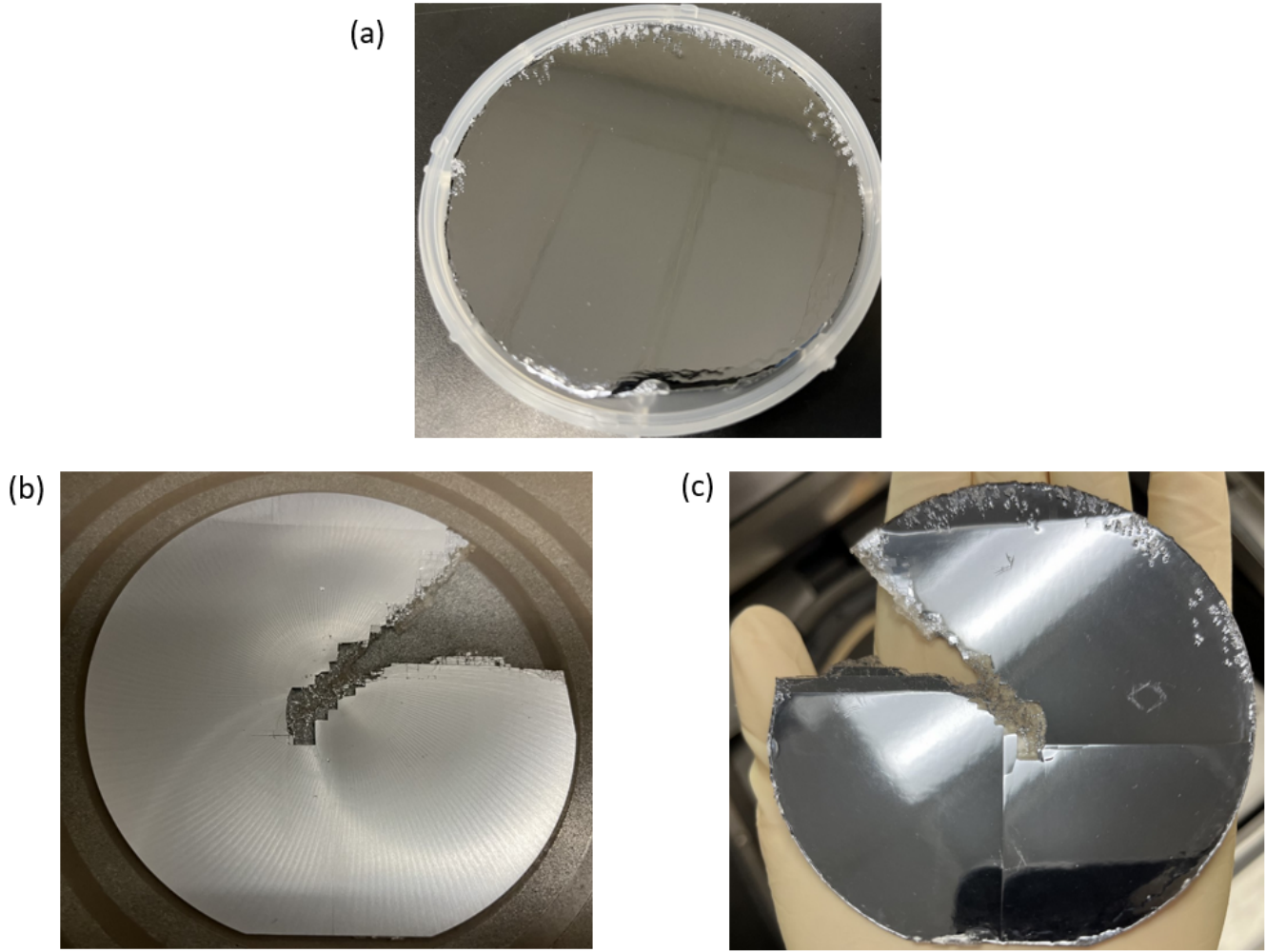


Figure 22: Experimental results of curing the PDMS on a leveled hotplate. (a) The cured PDMS is perfectly flat, although slightly slanted from one end of the wafer to the other. Bubbles have also been observed to form at the edges as a consequence of curing on a hotplate as opposed to an oven. (b) Backside and (c) front side of the wafer post-grind failure and subsequent manual removal of handle material stack, to expose the PDMS in the center of the sample.

### 3 Conclusions and Discussion

Although we were unable to complete the end-to-end process of manufacturing nanostructures embedded in a flexible material within the quarter, the results of our experiments and the processes we investigated, which are documented in SOPs and nanonuggets, serve as a solid foundation to continue this research. We demonstrated the feasibility of using a custom molding process to layer thick, stiff PDMS onto silicon wafers. Using SEM imaging, we also showed that the chosen formulation of PDMS, consisting of 1 part SYLGARD 184 base to 2 parts curing agent penetrate the microstructures of our optical metasurface readily. Finally, we demonstrated that backgrinding to remove the handle material stack is a feasible solution to releasing the elastomer-embedded nanostructures.

Further work is required to develop a robust wafer backgrinding removal process for the handle material stack. We are confident that using a thinner film of 1:2 ratio PDMS, in conjunction with removing the *spark-out* step from the backgrinding process, are sufficient steps to allow the process to work. The main reason for the premature failure of the backgrinding process in this study is the uneven application of force to a silicon wafer with a compressible superstrate. Thus, one potential solution is to switch away from the conventionally-used PDMS to a completely non-compressible, but still flexible, optical material. One such option is polymethyl methacrylate (PMMA). PMMA is a thermoplastic, which is not readily compressible at room temperature, allowing the backgrinding process to be completed, but moldable when heated, thus allowing it to be shaped into conformal shapes, similar to PDMS.

In this report, we pave the way for perfecting a process to quickly mass-manufacture embedded nano- and micro-structure devices, by carefully documenting the successes and failures of both conventional and newly-developed techniques for all stages of the manufacturing process. We have identified the root causes of the issues we faced, and laid out a plan to complete the process end-to-end. We are planning on continuing this research, to finalize a robust process for the mass-manufacturing of conformal optical metasurfaces. This report will be updated upon the completion of this study.

### 4 Acknowledgements

We would like to thank our advisor, Prof. Jonathan Fan, for his help in conceptualizing the process proposed in this report. We thank our mentors, J Provine, Swaroop Kommera, and Lavendra Mandyam, and all other E241 mentors, for their continued help and support throughout the quarter, helping us through the unconventional problems we faced during our unconventional experiments. We thank Prof. Roger Howe for his continued insight in helping us work through the challenges we encountered during the development of our experimental processes. We are also extremely grateful to the entire SNF staff and community of superusers, whose expertise and patience in training and advising us is invaluable.



## 5 Appendices

### 5.1 Processes developed to facilitate PDMS curing

Early on in the development of processes to cure PDMS on silicon wafers, it was determined that PDMS curing to the underside of the wafer posed a big problem. This is because cured PDMS on the underside of the wafer interfered both with film thickness and compression measurements post-curing and with the grinding process. Thus, a method was shared with us by our labmate, Peter Phan, and documented here, to remedy this problem. As illustrated in Fig. 23, it is completed in 5 steps:

1. Trace a circle on the back of *blue sticky tape* (stocked at SNF), that is slightly larger than the wafer being protected. The single wafer holder makes a great stencil.
2. Cut out the circle using scissors.
3. Cut a hole in the center of the circle cut-out, allowing for the vacuum chuck of the spinner to make contact with the underside of the wafer.
4. Carefully peel back the blue sticky tape.
5. Place the wafer on top of the blue sticky tape, and gently tap the edges using wafer tweezers to make sure the bond is tight.

After the PDMS is spun onto the wafer, the tape is removed using two wafer tweezers: one is used to hold the wafer from the edge, while the other is used to gently remove the tape.

### 5.2 Fine-grinding parameter selection

The optimal grinding parameters for fine, precise grinding were selected based on results from the literature [5] and from trial-and-error. Note that these parameters are not final, and are still in an experimental stage. For the final stages of grinding, please turn off *spark-out*, as this smooths the wafer through tensile stresses, and is likely to break extremely thin material stacks.

The parameters used for extreme thinning in this study are illustrated in Fig. 24. Note that 20% of the height is grinded away in stage 1, 40% in stage 2, and the remaining 40% in stage 3. These must be adjusted accordingly if the wafer is thinned in multiple rounds of grinding processes.

### 5.3 PDMS height via differential drop gauge measurement technique

An apparent issue with the use of the differential drop gauge to measure the thickness and compression amount of the cured films of PDMS is that the metal tip of the instrument easily damages the film. Furthermore, it does not provide an accurate measurement, as it digs into the film, thus not accurately measuring the height of the surface of the film, but rather a pressed height beneath

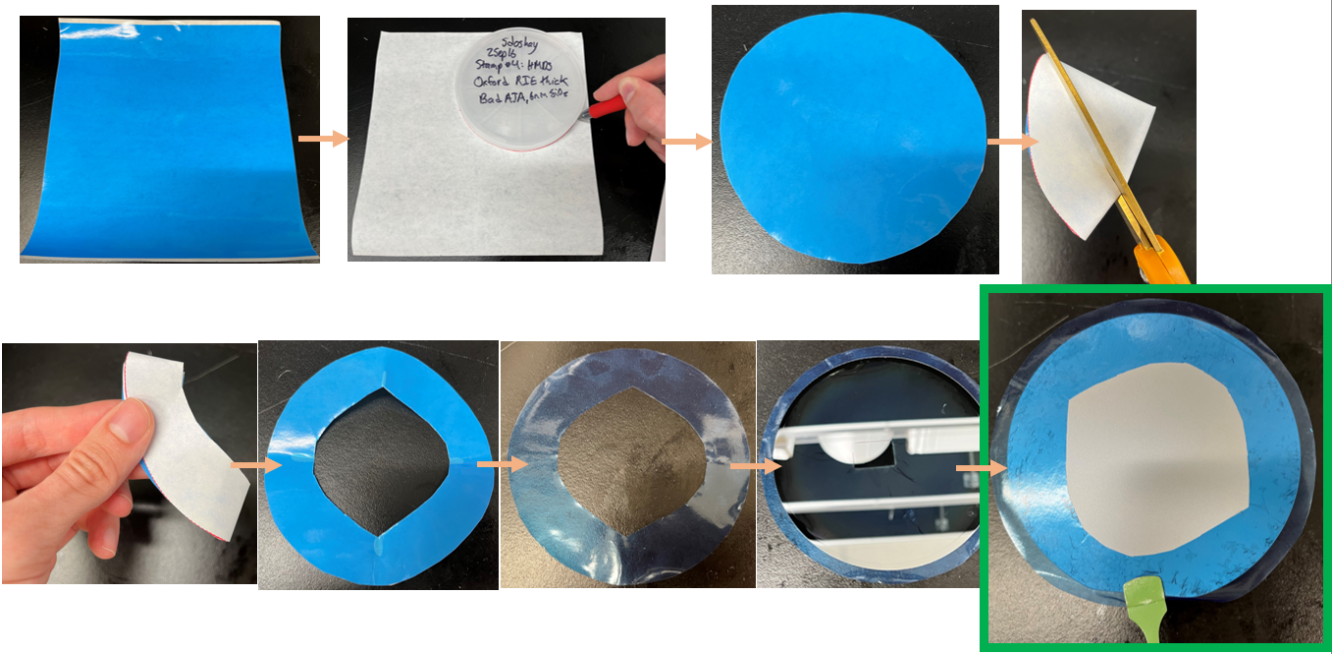


Figure 23: Step-by-step illustration of how to protect the backside of a wafer from PDMS during the spinning process.

the surface. Thus, a method was devised to accurately and measure the PDMS film height, as illustrated in Fig. 25. A small piece (5mm X 5mm) of cleaved silicon was determined to work very well. The piece must be small enough such that it can be easily removed after measurement is finished, but large enough such that the tip's force can be evenly distributed across an area of PDMS film that is large enough to prevent damage. It was also determined that it is best to keep the polished side of the measuring protective piece upwards, such that the rough side of the cleaved piece is touching the PDMS film. This prevents the easy surface bonding that occurs between polished silicon surfaces and PDMS. Thus, removing the protective piece after measurement is straightforward.

## 5.4 Budget

We spent a total of \$4923.84 out of a total budget of \$5000.00. The SYLGARD 184 was provided by our research advisor, Prof. Jonathan Fan. The largest expense of this project was the CVD, as this process required waiting for the furnace to cool for the smooth deposition of germanium, then heat for the deposition of polycrystal silicon, which results in expensive tool use time. The breakdown of the expenses is tabulated in Table 1.

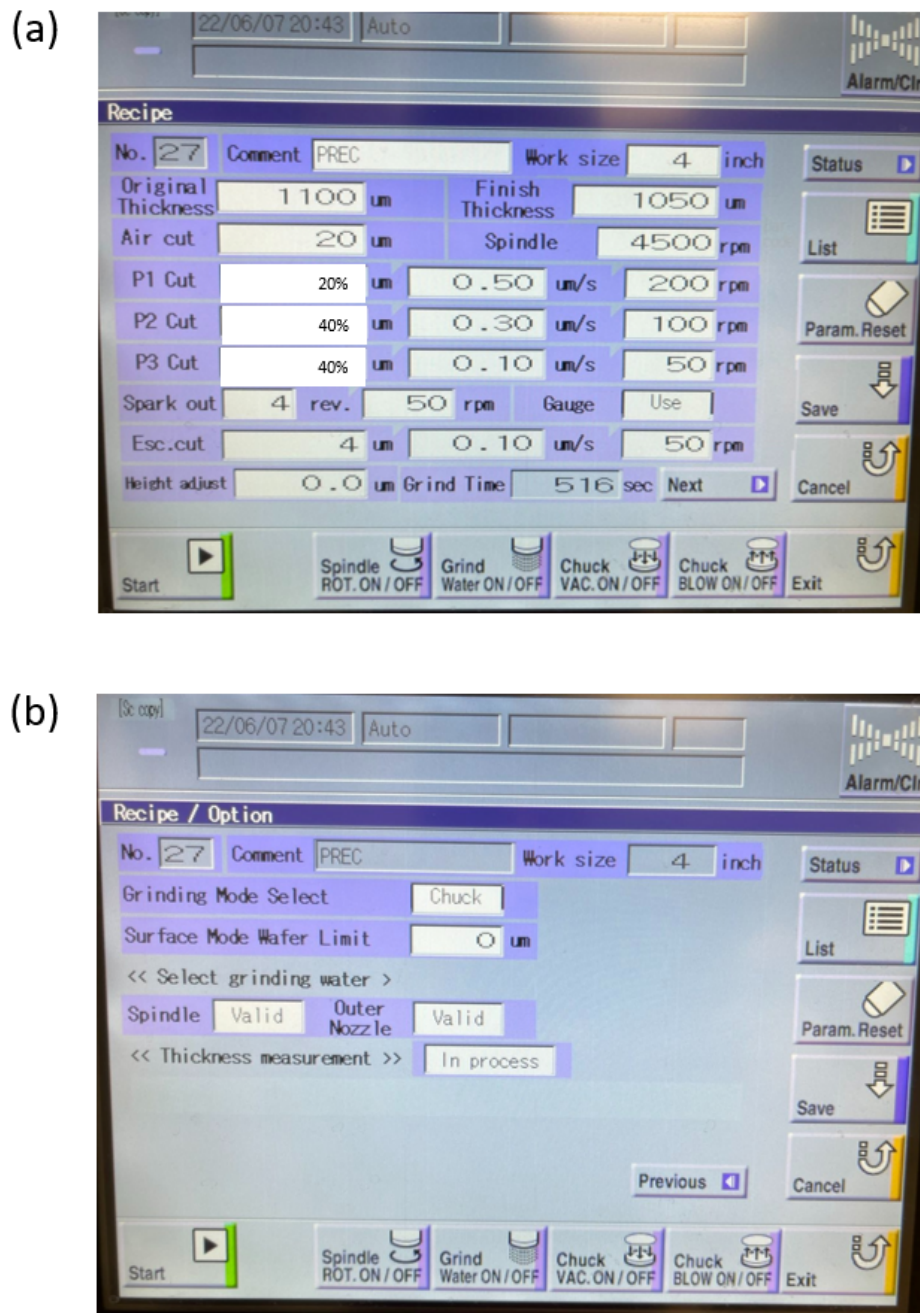


Figure 24: Semi-optimized grinding parameters for the fine and precise grinding of silicon wafers, demonstrated to stop to within 2 $\mu$ m of the intended target for both PDMS superstrate and no superstrate silicon wafers.



Figure 25: Drop gauge measurement with a protective silicon piece, used to protect the film from damage from the drop gauge tip.

Table 1: Budget summary

Item	Expense
Training	\$1330.00
Materials	\$756.00
Tool use	\$2835.84
Total	\$4921.84

## References

- [1] Controlled preparation of thermally stable fe-poly(dimethylsiloxane) composite by magnetic induction heating. *Polymers*, 10(5)(507), 2018.
- [2] Properties and applications of pdms for biomedical engineering: A review. *Journal of Functional Biomaterials*, 13(1)(2), 2022.
- [3] T. Baëtens and S. Arscott. Planarization and edge bead reduction of spin-coated polydimethylsiloxane. *Journal of Micromechanics and Microengineering*, 29(11):115005, aug 2019.
- [4] S. M. Kamali, E. Arbabi, A. Arbabi, and A. Faraon. A review of dielectric optical metasurfaces for wavefront control. *Nanophotonics*, 7(6):1041–1068, 2018.

- [5] Z. Pei and A. Strasbaugh. Fine grinding of silicon wafers: designed experiments. *International Journal of Machine Tools and Manufacture*, 42(3):395–404, 2002.